

Ab Initio Investigation of the Electronic Structure and Bonding of the $\text{HC}(\text{N}_2)_x^+$ and $\text{HC}(\text{CO})_x^+$ Cations, $x = 1, 2$

Aristotle Papakondylis*[†] and Aristides Mavridis*[‡]

Laboratory of Physical Chemistry, Department of Chemistry, National and Kapodistrian University of Athens, P.O. Box 64 004, 157 10 Zografou, Athens, Greece

Received: March 21, 2005; In Final Form: April 28, 2005

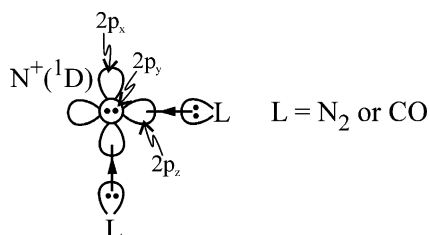
Employing the coupled-cluster approach and correlation consistent basis sets of triple and quadruple cardinality, we have investigated the electronic structure and bonding of the $\text{HC}(\text{N}_2)_x^+$ and $\text{HC}(\text{CO})_x^+$, $x = 1, 2$, molecular cations. We report geometries, binding energies and potential energy profiles. The ground states of $\text{HC}(\text{N}_2)^+$, $\text{HC}(\text{CO})^+$ and $\text{HC}(\text{N}_2)_2^+$, $\text{HC}(\text{CO})_2^+$ are of $^3\Sigma^-$ and 1A_1 symmetries, respectively. All four charged species are well bound with binding energies ranging from 81 [$\text{HC}(\text{N}_2)^+ (\tilde{X}^3\Sigma^-) \rightarrow \text{CH}^+(a^3\Pi) + \text{N}_2(X^1\Sigma_g^+)$] to 178 [$\text{HC}(\text{CO})_2^+(\tilde{X}^1A_1) \rightarrow \text{CH}^+(X^1\Sigma^+) + 2\text{CO}(X^1\Sigma^+)$] kcal/mol. It is our belief that the \tilde{X}^1A_1 states of $\text{HC}(\text{N}_2)_2^+$ and $\text{HC}(\text{CO})_2^+$ are isolable in the solid state if combined with appropriate counteranions.

1. Introduction

In 1999, the isolation of the N_5^+ ($=\text{N}(\text{N}_2)_2^+$) species by Christe and co-workers¹ attracted the attention of the world molecular scientists. This polynitrogen cationic entity properly protected by bulky counteranions can be stored at low temperature without noticeable decomposition. Almost at the same time Seppelt et al.² announced the isolation (as a salt) of the $\text{N}(\text{CO})_2^+$ cation, isoelectronic and isoivalent to $\text{N}(\text{N}_2)_2^+$, whose stability exceeds that of $\text{N}(\text{N}_2)_2^+$. The $\text{N}(\text{CO})_2^+$ species had already been observed in the gas phase since 1992.³

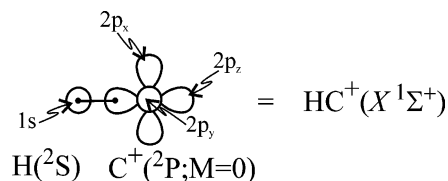
Three years ago, we presented a thorough theoretical analysis on both these cationic systems in an effort to understand their bonding character.⁴ It was clearly shown that the binding is the result of σ -charge transfer from N_2 or CO , to the available 2p orbitals of the in situ excited $\text{N}^+(^1D; 2s^22p^2)$ atom. The valence-bond-Lewis (vbL) icon shown in Scheme 1 clearly captures the

SCHEME 1

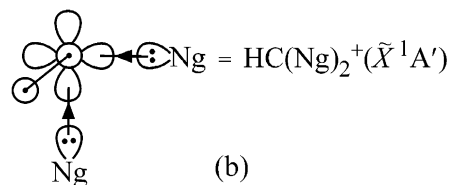
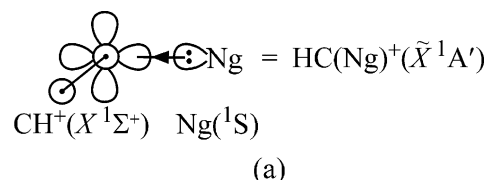


bonding scenario, where the first excited state of N^+ (1D) lies 1.888 eV above its ground 3P state.⁵ Scheme 1 suggests the existence of a plethora of similar type stable compounds by mere replacing the N_2 or CO ligands with any electron donor group (see ref 4). Another possibility is the replacement of the central N^+ cation by a molecular entity having similar electronic distribution as the 1D term of N^+ , and, of course, preferably being in the ground state. In a recent paper,⁶ we showed that CH^+ , the ground state of which is graphically shown in Scheme 2, is a good candidate.

SCHEME 2



SCHEME 3



Clearly $\text{CH}^+(X^1\Sigma^+)$ carries the same binding sites as the 1D state of N^+ , but with the advantage of being in the ground state.

In ref 6, we examined by coupled cluster methods the ability of noble gas atoms (Ng) to form stable singlet $\text{HC}(\text{Ng})_x^+$ cationic species, where $x = 1, 2$ and $\text{Ng} = \text{He}, \text{Ne}, \text{Ar}, \text{Kr},$ and Xe . Our calculations revealed considerably strong $\text{HC}^+ \leftarrow \text{:Ng}$ “dative” bonds, particularly when $\text{Ng} = \text{Ar}, \text{Kr},$ and Xe . In all cases the in situ CH^+ finds itself in the $X^1\Sigma^+$ state whereas the binding can be faithfully represented by the vbL diagrams shown in Scheme 3 (see also Scheme 2).

The Scheme 3 diagrams predict strongly bent geometries of the $\text{HC}(\text{Ng})^+$ series and an almost perpendicular C–H bond to the NgCNg plane in the $\text{HC}(\text{Ng})_2^+$ case, in complete agreement with our calculations.⁶

In what follows we present highly correlated ab initio calculations on the interaction of CH^+ with $\text{L} = \text{N}_2$ and CO .

[†] E-mail: papakondylis@chem.uoa.gr.

[‡] E-mail: mavridis@chem.uoa.gr

TABLE 1: Total Energies E (hartree), Bond Lengths (\AA), Harmonic Frequencies ω_e (cm^{-1}), Separation Energies T_e (cm^{-1}), and Electron Affinities EA (eV) or Ionization Energies IE (eV) of Four Electronic States of CH^+ and the Ground States of N_2 and CO at the RCCSD(T)/cc-pVTZ Level of Theory, with Experimental Values in Parentheses

species	$-E$	r_e	ω_e	T_e	EA
CH^+ ($X^1\Sigma^+$)	38.02362	1.1311 (1.1309) ^a	2849.5 (2857.56) ^a	0	10.52 (10.64) ^b
CH^+ ($a^3\Pi$)	37.98010	1.1358	2690.1 (2814.0) ^c	9550.4	
CH^+ ($b^3\Sigma^-$)	37.84760	1.2449 (1.2446) ^b	2058.6	39 661 (38200) ^c	
CH^+ ($B^1\Delta$) ^d	37.77972	1.2271 (1.2325) ^b		53 529 (52534) ^c	

species	$-E$	r_e	ω_e	T_e	IE
N_2 ($X^1\Sigma_g^+$)	109.37394	1.1038 (1.0977) ^b	2345.8 (2358.6) ^b	0.0	15.43 (15.58) ^b
CO ($X^1\Sigma^+$)	113.15558	1.1357 (1.1283) ^b	2153.6 (2169.8) ^b	0.0	13.90 (14.01) ^b

^a Reference 12. ^b Reference 13. ^c Reference 13, uncertain values.

^d The $B^1\Delta$ state of CH^+ (A_1 component) was obtained by pulling apart the two N_2 (or CO) ligands of the X^1A_1 state of $\text{HC}(\text{N}_2)_2^+$ (or $\text{HC}(\text{CO})_2^+$) and optimizing the C–H bond distance at infinity; see section 3 and Figures 3 and 4.

Note that the $\text{HC}(\text{CO})_2^+$ molecular cation has been observed since 1998 in the gas phase by mass spectrometric methods.⁷ For the $\text{HC}(\text{N}_2)_x^+$ and $\text{HC}(\text{CO})_x^+$ molecules we report total

energies, geometries, binding energies, harmonic frequencies and potential energy profiles. We also compare our findings with the $\text{N}(\text{N}_2)_x^+$, $\text{N}(\text{CO})_x^+$, and $\text{HC}(\text{N}_2)_x^+$ molecular cations previously studied.^{4,6} To the best of our knowledge this is the first time that these systems are examined theoretically in a systematic and thorough manner.

2. Computational Outline

All our calculations were performed using the coupled cluster singles and doubles (CCSD) with a perturbative treatment of connected triple excitations [CCSD(T)] methodology.⁸ For the triplet states the restricted variant based on a restricted open-shell Hartree–Fock reference, RCCSD(T) method, was employed.⁹ Through all calculations only valence electrons were correlated. The CC-single reference approach is ideal for describing purely dative (harpoon-like) bonds of the type shown in Scheme 3, parts a and b. Indeed, we were able to construct full potential energy profiles of the reactions $\text{HC}^+ + x\text{L} \rightarrow \text{HCL}_x^+$, $\text{L} = \text{N}_2$ and CO , at the RCCSD(T) level of theory.

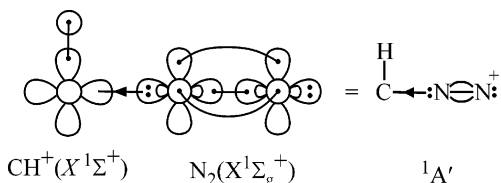
The plain correlation consistent triple- ζ , cc-pVTZ basis set of Dunning¹⁰ generally contracted to [4s3p2d1f/c_{N,O} 3s2p1d/H] was used to obtain potential energy curves, geometries and harmonic frequencies. However, the HC-L_x^+ binding energies were recalculated at the RCCSD(T)/cc-pVQZ level using the cc-pVTZ geometries, RCCSD(T)/cc-pVQZ/cc-pVTZ. Our largest calculations on the HCL_2^+ systems number 305 spherical Gaussian orbital functions. Finally, equilibrium geometries and

TABLE 2: Total Energies E (hartree), Binding Energies D_e and D_0 (kcal/mol), Separation Energies T_e (kcal/mol), Geometries (in \AA and deg), and Mulliken Charges (Numbers in Parentheses) of the $X^3\Sigma^-$ and a^1A' States of $\text{HC}(\text{N}_2)^+$, and $\text{HC}(\text{CO})^+$ at the RCCSD(T)/cc-pVTZ//RCCSD(T)/cc-pVQZ Level

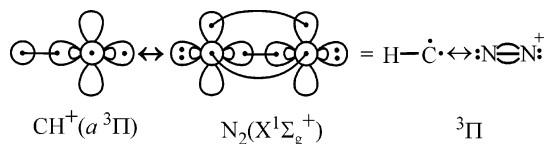
State	Basis Set	$-E$	D_e	D_0^a	T_e	Bond Lengths, Bond Angles and Hartree-Fock Net Mulliken Charges
$\text{HC}^+(\text{N}_2)$						
$X^3\Sigma^-$	cc-pVTZ	147.48222	80.4 ^c 163.6 ^d	78.2 ^c 160.4 ^d	0.0	$\begin{array}{cccc} 1.082 & 1.208 & 1.190 & \\ \text{H} & \text{---C} & \text{---N} & \text{---N} \\ (+0.34) & (+0.29) & (+0.19) & (+0.18) \end{array}$
	cc-pVQZ ^b	147.51966	81.2 ^c 164.3 ^d	– –	0.0	
a^1A'	cc-pVTZ	147.46282	41.0 ^e	37.5 ^e	12.2	$\begin{array}{cccc} & (+0.24) & & \\ & \text{H} & & \\ & 1.108 & 104.8^\circ & (+0.23) \\ (+0.24) & \text{C} & \text{---N} & \text{---N} \\ & 1.426 & 165.4^\circ & 1.118 \\ & & & (+0.29) \end{array}$
	cc-pVQZ ^b	147.50036	41.3 ^e	–	12.1	
$\text{HC}^+(\text{CO})$						
$X^3\Sigma^-$	cc-pVTZ	151.31947	115.3 ^f 198.5 ^g	114.7 ^f 193.1 ^g	0.0	$\begin{array}{cccc} 1.081 & 1.326 & 1.143 & \\ \text{H} & \text{---C} & \text{---C} & \text{---O} \\ (+0.30) & (+0.14) & (+0.50) & (+0.06) \end{array}$
	cc-pVQZ ^b	151.35927	116.4 ^f 199.5 ^g	– –	0.0	
a^1A'	cc-pVTZ	151.28956	69.2 ^h	65.0 ^h	18.8	$\begin{array}{cccc} & (+0.26) & & \\ & \text{H} & & \\ & 1.100 & 114.4^\circ & (+0.49) \\ (+0.13) & \text{C} & \text{---C} & \text{---O} \\ & 1.436 & 165.1^\circ & 1.134 \\ & & & (+0.11) \end{array}$
	cc-pVQZ ^b	151.32960	70.0 ^h	–	18.6	

^a Zero-point energy corrected binding energies. Harmonic frequencies are available upon request. ^b Using the CCSD(T)/cc-pVTZ optimized geometries. ^c With respect to $\text{CH}^+(a^3\Pi) + \text{N}_2(X^1\Sigma_g^+)$. ^d With respect to $\text{CH}^+(b^3\Sigma^-) + \text{N}_2(X^1\Sigma_g^+)$. ^e With respect to $\text{CH}^+(X^1\Sigma^+) + \text{N}_2(X^1\Sigma_g^+)$. ^f With respect to $\text{CH}^+(a^3\Pi) + \text{CO}(X^1\Sigma^+)$. ^g With respect to $\text{CH}^+(b^3\Sigma^-) + \text{CO}(X^1\Sigma^+)$. ^h With respect to $\text{CH}^+(X^1\Sigma^+) + \text{CO}(X^1\Sigma^+)$.

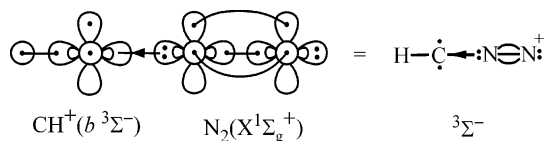
SCHEME 4



SCHEME 5



SCHEME 6



harmonic frequencies were determined by complete optimization and Hessian matrix diagonalization, respectively.

All calculations were carried out with the MOLPRO2002.6 code.¹¹

3. Results and Discussion

Numerical results of four electronic states of CH⁺ ($X^1\Sigma^+$, $a^3\Pi$, $b^3\Sigma^-$, $B^1\Delta$) entailed in the HCL_x⁺ study, as well as results on the ground states of N₂ and CO molecules at the RCCSD(T)/cc-pVTZ level, under C_{2v} symmetry constraints, are collected in Table 1. All calculated properties are consistent with existing experimental values.

HC(N₂)⁺, HC(CO)⁺. Table 2 lists our results on the HC(N₂)⁺ and HC(CO)⁺ systems. Considering the $X^1\Sigma^+$, $a^3\Pi$, and $b^3\Sigma^-$ states of CH⁺, we can envisage at least three routes of interaction of CH⁺ with N₂ or CO, explicated by vBL diagrams (Schemes 4–6).

Identical vBL diagrams can be drawn with CO($X^1\Sigma^+$) instead of N₂. In addition, from Scheme 5, it is clear that N₂ can approach the CH⁺ $a^3\Pi$ state perpendicularly to the C–H axis and along the empty p_π orbital leading to a bonding interaction of $^3A''$ symmetry (but see below). Scheme 4 predicts a strongly bent state with the in situ N₂ moiety more or less intact, Scheme 5 leads to a linear repulsive or weakly bound state, while Scheme 6 suggests a linear $^3\Sigma^-$ state much more strongly bound than $^1A'$, with a shorter C–N and a longer N–N bond distance as compared to the $^1A'$ state. The cause of these expectations concerning the $b^3\Sigma^-$ state is that the σ-density of N₂ faces a less shielded carbon atom (remember, the in situ CH⁺ in the $b^3\Sigma^-$ state correlates to C⁺ ($2s^1 2p^2; ^4P$, M = 0) and, also, due to the strong “conjugation” of the three π_x and π_y electrons. Obviously, Schemes 4–6 and corresponding inferences carry the same to CO($X^1\Sigma^+$).

The numbers in Table 2 and the potential energy profiles in Figures 1 and 2 with both N₂ and CO molecules are in complete agreement with the analysis above. What perhaps is surprising, is that the ground states of HC(N₂)⁺ and HC(CO)⁺ are of $^3\Sigma^-$ symmetry, considering that the $b^3\Sigma^-$ state of CH⁺ is about 5 eV above its $X^1\Sigma^+$ state (Table 1). The situation is different from the HC(Ng)⁺ series (Ng = Noble gas), where we have \tilde{X}^1A' ground states⁶ shown schematically in (3a), but resembles the isoelectronic cations N₃⁺($\tilde{X}^3\Sigma_g^-$) and NCO⁺($\tilde{X}^3\Sigma^-$).⁴

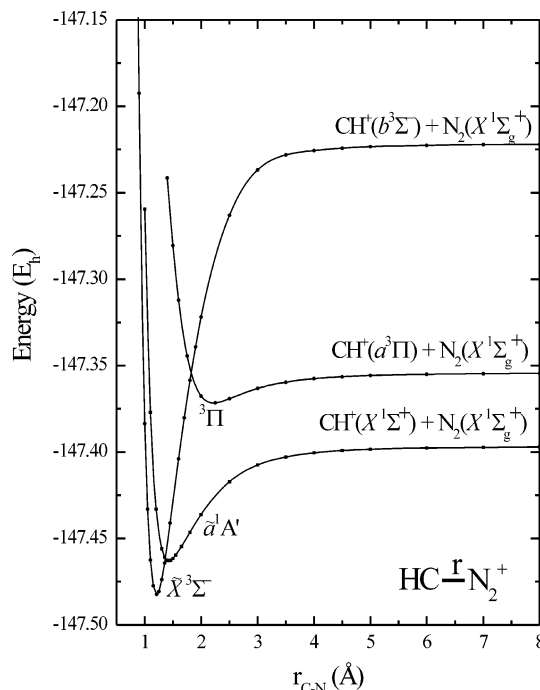


Figure 1. Potential energy profiles of the CH⁺($X^1\Sigma^+$, $a^3\Pi$, $b^3\Sigma^-$) + N₂($X^1\Sigma_g^+$) channels at the RCCSD(T)/cc-pVTZ level of theory. The HCN–N bond distance was kept fixed at its equilibrium value; the H–CN₂ bond distance was smoothly varied from its equilibrium value to the value of the corresponding free CH⁺ state.

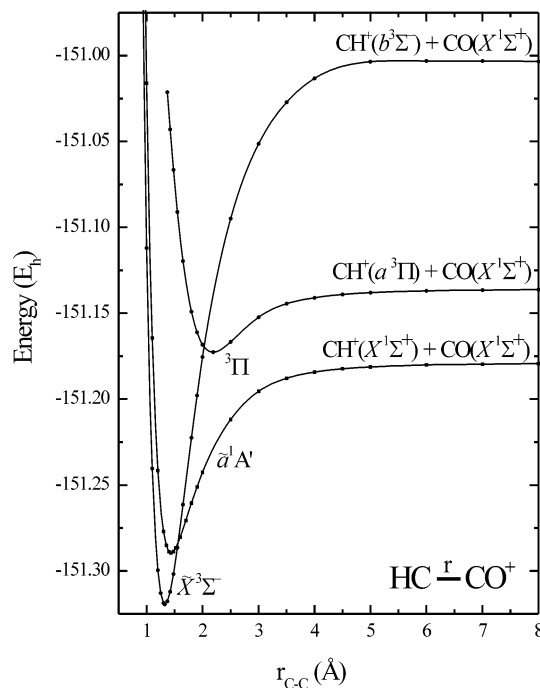
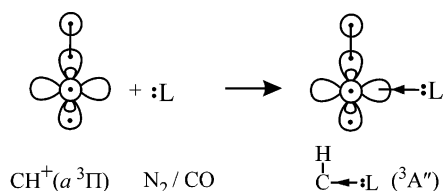


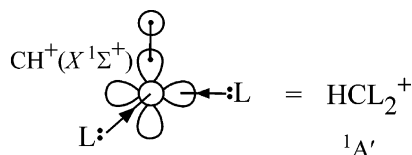
Figure 2. Potential energy profiles of the CH⁺($X^1\Sigma^+$, $a^3\Pi$, $b^3\Sigma^-$) + CO($X^1\Sigma^+$) channels at the RCCSD(T)/cc-pVTZ level of theory. The HCC–O bond distance was kept fixed at its equilibrium value; the H–CCO bond distance was smoothly varied from its equilibrium value to the value of the corresponding free CH⁺ state.

Let us examine now in some detail the potential energy curves for the linear approaches CH⁺($a^3\Pi$, $b^3\Sigma^-$) + N₂($X^1\Sigma_g^+$) and CO($X^1\Sigma^+$) shown in Figures 1 and 2 (see also Schemes 5 and 6). These curves are “slices” of the potential energy hypersurfaces \tilde{X}^3A'' and \tilde{A}^3A'' of the HC(N₂)⁺ and HC(CO)⁺ systems. The $\tilde{X}^3\Sigma^-$ states are global minima of the related \tilde{X}^3A'' surfaces which correlate asymptotically to the CH⁺($a^3\Pi$) + N₂($X^1\Sigma_g^+$)

SCHEME 7



SCHEME 8



or $\text{CO}(X^1\Sigma^+)$ channels. These surfaces suffer a conical intersection with the upper \tilde{A}^3A'' surfaces, indicated by the crossing of the ${}^3\Sigma^-$ and ${}^3\Pi$ curves for the linear geometries at a C–N₂ or C–CO bond distance of about 2 Å. The \tilde{A}^3A'' potential surfaces correlate to the $\text{CH}^+(b^3\Sigma^-) + \text{N}_2(X^1\Sigma_g^+)$ or $\text{CO}(X^1\Sigma^+)$ end products. On the ground \tilde{X}^3A'' no other local minima were found as one could have expected considering the interaction shown in Scheme 7, which leads to a bent ${}^3A''$ structure (compare also

Scheme 5). In fact, what happens is that this ${}^3A''$ structure decays barrierlessly to the linear ${}^3\Sigma^-$ ground state by relaxing the $\angle\text{HCL}$ angle.

The binding energies of $\text{HC}(\text{N}_2)^+(\tilde{X}^3\Sigma^-)/\text{HC}(\text{CO})^+(\tilde{X}^3\Sigma^-)$ with respect to $\text{CH}^+(a^3\Pi) + \text{N}_2(X^1\Sigma_g^+)/\text{CO}(X^1\Sigma^+)$ products are $D_e = 81.2/116.4$ kcal/mol at the RCCSD(T)/cc-pVQZ level. However, the intrinsic HC–L bond strength, i.e., with respect to $\text{CH}^+(b^3\Sigma^-) + \text{N}_2(X^1\Sigma_g^+)/\text{CO}(X^1\Sigma^+)$ is much higher, 164.3/199.5 kcal/mol, respectively; see Table 2.

In Figures 1 and 2, the potential energy curves of the singlet ${}^1A'$ states are displayed corresponding to Scheme 4. From Table 2 we see that these \tilde{a}^1A' states of HCL^+ lie 12.1 and 18.6 kcal/mol higher than the $\tilde{X}^3\Sigma^-$ ground states for L = N₂ and CO, respectively. They have strongly bent geometries, $\angle\text{HCL} = 104.8^\circ$ and 114.4° , in conformity with the vbL diagram (Scheme 4).

$\text{HC}(\text{N}_2)_2^+$, $\text{HC}(\text{CO})_2^+$. From the previous discussion on the HCL^+ cations it is clear that the addition of a second L (N₂ or CO) ligand to the $\tilde{X}^3\Sigma^-$ state of HCL^+ , could only result in a weakly bound electrostatic $\text{HCL}^+\cdots\text{L}$ system (Scheme 6). It is seen however that the \tilde{a}^1A' states (Scheme 4) offer the possibility for the attachment of a second substituent L (N₂ or CO) to the empty p_π orbital according to Scheme 8.

TABLE 3: Total Energies E (hartree), Binding Energies D_e and D_0 (kcal/mol), Geometries (in Å and deg), and Mulliken Charges (Numbers in Parentheses) of the $\text{HC}(\text{N}_2)_2^+$, $\text{HC}(\text{CO})_2^+$, and $\text{HC}(\text{N}_2)(\text{CO})^+$ at the RCCSD(T)/cc-pVTZ/RCCSD(T)/cc-pVQZ Level of Theory

Basis Set	– E	D_e	D_0^a	Bond Lengths, Bond Angles and Hartree-Fock Net Mulliken Charges	
$\text{HC}^+(\text{N}_2)_2 (X^1A_1)$					
cc-pVTZ	256.91122	46.7 ^b 87.7 ^c	41.4 ^b 78.9 ^c		
cc-pVQZ ^d	256.98074	47.7 ^b 89.0 ^c	–	–	
$\text{HC}^+(\text{CO})_2 (X^1A_1)$					
cc-pVTZ	264.61609	107.3 ^e 176.5 ^f	101.7 ^e 162.7 ^f		
cc-pVQZ ^d	264.69019	108.4 ^e 178.4 ^f	–	–	
$\text{HC}^+(\text{CO})(\text{N}_2) (X^1A')$					
cc-pVTZ	260.76353	62.8 ^g 91.1 ^h 132.0 ⁱ	–		
cc-pVQZ ^d	264.69019	63.6 ^g 92.3 ^h 133.6 ⁱ	–	–	

^a Zero-point energy corrected binding energies with harmonic frequencies of $\text{HC}^+(\text{N}_2)_2 (\tilde{X}^1A_1)$ and $\text{HC}^+(\text{CO})_2 (\tilde{X}^1A_1)$: {169.8, 334.7, 375.5, 468.8, 495.9, 620.6, 1024.8, 1157.1, 1325.8, 2174.4, 2270.2, 3278.6} cm^{-1} and {149.7, 419.5, 448.4, 541.2, 593.0, 660.7, 996.4, 1117.5, 1387.5, 2241.4, 2326.1, 3186.1} cm^{-1} , respectively. ^b With respect to $\text{HC}^+(\text{N}_2) (\tilde{X}^1A_1) + \text{N}_2(X^1\Sigma_g^+)$. ^c With respect to $\text{CH}^+(X^1\Sigma^+) + 2\text{N}_2(X^1\Sigma_g^+)$. ^d Using the CCSD(T)/cc-pVTZ optimized geometries. ^e With respect to $\text{HC}^+(\text{CO}) (\tilde{X}^1A_1) + \text{CO}(X^1\Sigma^+)$. ^f With respect to $\text{CH}^+(X^1\Sigma^+) + 2\text{CO}(X^1\Sigma^+)$. ^g With respect to $\text{HC}^+(\text{CO}) (\tilde{X}^1A_1) + \text{N}_2(X^1\Sigma_g^+)$. ^h With respect to $\text{HC}^+(\text{N}_2) (\tilde{X}^1A_1) + \text{CO}(X^1\Sigma^+)$. ⁱ With respect to $\text{CH}^+(X^1\Sigma^+) + \text{N}_2(X^1\Sigma_g^+) + \text{CO}(X^1\Sigma^+)$.

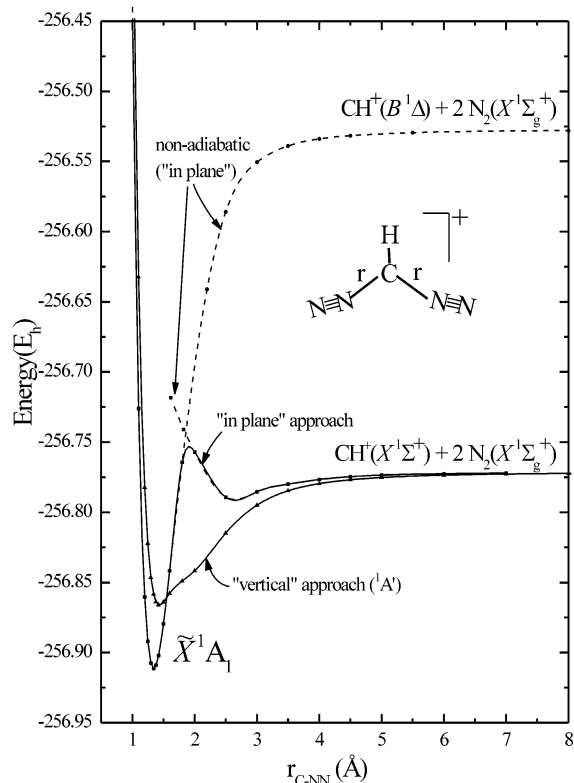


Figure 3. Potential energy profiles of the reaction $\text{CH}^+(\text{X}^1\Sigma^+) + 2\text{N}_2(\text{X}^1\Sigma_g^+) \rightarrow \text{HC}(\text{N}_2)_2^+(\tilde{\text{X}}^1\text{A}_1)$ at the RCCSD(T)/cc-pVTZ level. For details, see text.

The vbL diagram (Scheme 8) suggests a pyramidal structure with the C–H bond more or less perpendicular to the LCL plane. Of course cross structures can arise if the two L molecules are different, L and L'.

The results of our calculations shown in Table 3 predict stable $\text{HC}(\text{N}_2)_2^+$, $\text{HC}(\text{CO})_2^+$, and $\text{HC}(\text{N}_2)(\text{CO})^+$ molecules, but with planar geometries belonging to the point groups C_{2v} (identical L's, $\tilde{\text{X}}^1\text{A}_1$) or C_s (different L's, $\tilde{\text{X}}^1\text{A}'$). The geometrical structures presented in Table 3 were obtained after minimization at the CCSD(T)/cc-pVTZ level, starting from the pyramidal conformers (Scheme 8) and are the global and only minima of the HCL_2^+ ($\tilde{\text{X}}^1\text{A}'$) hypersurfaces. The reason that the HCL_2^+ (or $\text{HCL}'\text{L}^+$) molecular cations are planar, instead of pyramidal as the vbL diagram (Scheme 8) implies, can be rationalized by examining Figures 3 and 4. These figures display potential energy profiles for the dissociation process $\text{HCL}_2^+(\tilde{\text{X}}^1\text{A}') \rightarrow \text{CH}^+(\text{X}^1\Sigma^+) + 2\text{L}(\text{X}^1\Sigma_g^+)$ by pulling apart the two L's in a symmetric fashion and conserving the planar C_{2v} geometry ("in plane" approach). We also show analogous curves but with the C–H bond forming a 90° angle with the LCL plane and under C_s restrictions ("vertical" approach; Scheme 8). It is seen that the "in plane" curves for both $\text{L} = \text{N}_2$ and CO cases undergo an avoided crossing at $r_{\text{C-L}} \approx 2 \text{ \AA}$. The nonadiabatic potential curves (dashed lines) obtained by "locking" the Hartree–Fock reference to the equilibrium geometry (planar) configuration are revealing: they correlate to the $\text{CH}^+(\text{B}^1\Delta) + \text{N}_2(\text{X}^1\Sigma_g^+)$ or $\text{CO}(\text{X}^1\Sigma^+)$ asymptotic products. The vbL diagram (Scheme 9) gives a succinct representation of the bonding.

The σ -density of the two L ligands interacts attractively with the two empty orbitals of $\text{CH}^+(\text{B}^1\Delta)$ leading to planar geometries. As indicated the in situ CH^+ is in the $\text{B}^1\Delta$ state lying 153 kcal/mol above its $\text{X}^1\Sigma^+$ state (Table 1). The binding energies D_e with respect to the ground-state fragments $\text{CH}^+(\text{X}^1\Sigma^+) + 2\text{N}_2(\text{X}^1\Sigma_g^+)/2\text{CO}(\text{X}^1\Sigma^+)$ are 89/178.4 kcal/mol at the

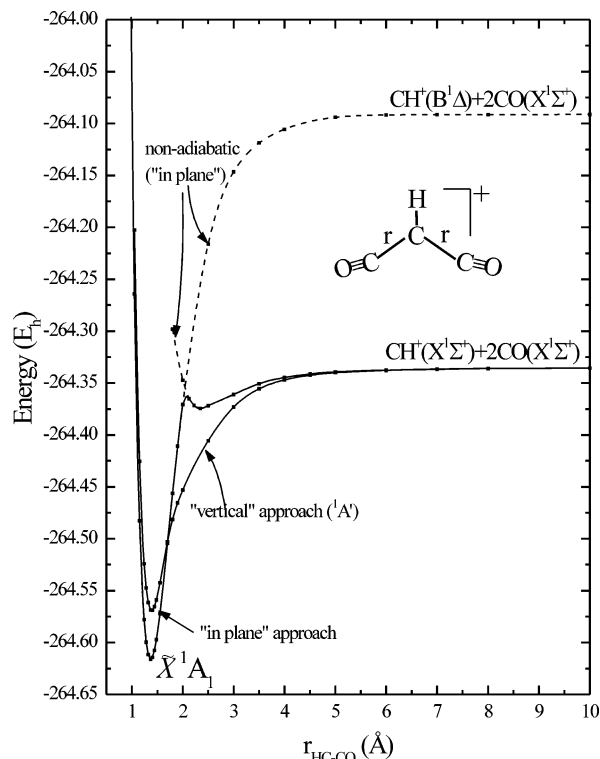
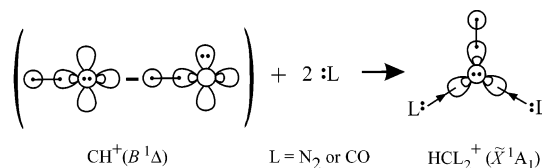


Figure 4. Potential energy profiles of the reaction $\text{CH}^+(\text{X}^1\Sigma^+) + 2\text{CO}(\text{X}^1\Sigma^+) \rightarrow \text{HC}(\text{CO})_2^+(\tilde{\text{X}}^1\text{A}_1)$ at the RCCSD(T)/cc-pVTZ level. For details, see text.

SCHEME 9



CCSD(T)/cc-pVQZ level. However, the intrinsic bond strengths, i.e., with respect to $\text{CH}^+(\text{B}^1\Delta) + 2\text{N}_2(\text{X}^1\Sigma_g^+)/2\text{CO}(\text{X}^1\Sigma^+)$ are 242/332 kcal/mol. Certainly the exposed carbon core of CH^+ in the $\text{B}^1\Delta$ state ($\text{C}^+(2s^12p^2; ^1\text{D})$) causes this enormous stabilization by strongly attracting the two electron σ -pairs of N_2 or CO . Indeed, the (Hartree–Fock) Mulliken population analysis indicates that the charge on the in situ CH moiety is almost completely quenched after interacting with the two N_2 or CO groups. The mechanism of formation of both $\text{HC}(\text{N}_2)_2^+$ and $\text{HC}(\text{CO})_2^+$ molecules can be viewed as a two step process (see also Figures 3 and 4): first a "vertical" attack of N_2 or CO on $\text{CH}^+(\text{X}^1\Sigma^+)$ to sidestep the energy barrier, followed by a relaxation step to the planar geometry. A similar two step mechanism was found in the case of formation of diazomethane, $\text{CH}_2(\tilde{\text{a}}^1\text{A}_1) + \text{N}_2(\text{X}^1\Sigma_g^+) \rightarrow \text{CH}_2\text{N}_2(\tilde{\text{X}}^1\text{A}_1)$, where the $\tilde{\text{c}}^1\text{A}_1$ state of CH_2 is involved.^{14,15}

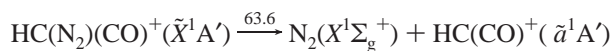
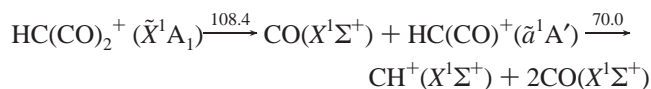
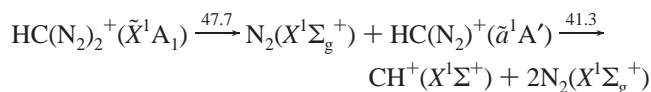
Finally, in Table 3 we also report numerical results for the mixed molecular cation $\text{HC}(\text{N}_2)(\text{CO})^+$. Similarly to the HCL_2^+ systems its ground state ($\tilde{\text{X}}^1\text{A}'$) has a planar geometrical structure. Interestingly enough the dissociation energy of the $\text{HC}(\text{N}_2)(\text{CO})^+$ with respect to the ground-state products $\text{CH}^+(\text{X}^1\Sigma^+) + \text{N}_2(\text{X}^1\Sigma_g^+) + \text{CO}(\text{X}^1\Sigma^+)$ is $D_e = 133.6$ kcal/mol at the CCSD(T)/cc-pVQZ level, exactly the mean value of the corresponding D_e 's of $\text{HC}(\text{N}_2)_2^+$ and $\text{HC}(\text{CO})_2^+$, $(89.0 + 178.4)/2 = 133.7$ kcal/mol; see Table 3.

4. Summary and Remarks

We have explored the geometric and electronic structure of the molecular cations HCL_x^+ , where $x = 1, 2$ and $L = \text{N}_2$ and CO , using coupled-cluster methods in conjunction with triple and quadruple quality correlation consistent basis sets. We report geometries, binding energies, and certain parts of the potential energy surfaces. Our main conclusions are epitomized below.

The $\text{HC}(\text{N}_2)^+$ and $\text{HC}(\text{CO})^+$ species are linear with ground states of $^3\Sigma^-$ symmetry and large $\text{HC}-\text{N}_2/\text{HC}-\text{CO}$ binding energies. Their similarity with the isoelectronic and isoivalent N_3^+ and NCO^+ cations is, indeed, interesting.⁴

The $\text{HC}(\text{N}_2)_2^+$ and $\text{HC}(\text{CO})_2^+$ cationic systems have planar C_{2v} geometries and 1A_1 ground states. The same holds true for the mixed species $\text{HC}(\text{N}_2)(\text{CO})^+$, but with a ground state of $^1A'$ symmetry. We indicate here the stability of those systems by showing their sequential dissociation energies (kcal/mol) at the CCSD(T)/cc-pVQZ level of theory.



In all three cations, $\text{HC}(\text{N}_2)_2^+$, $\text{HC}(\text{CO})_2^+$, and $\text{HC}(\text{N}_2)(\text{CO})^+$, the in situ CH^+ entity finds itself in the $B^1\Delta$ excited state.

Finally, we would like to point out the remarkable resemblance of $\text{HC}(\text{N}_2)_2^+$ and $\text{HC}(\text{CO})_2^+$ molecules with their

isoelectronic and isoivalent counterparts $\text{N}(\text{N}_2)_2^+$ and $\text{N}(\text{CO})_2^+$; see ref 4. We believe that the $\text{HC}(\text{N}_2)_2^+$ and $\text{HC}(\text{CO})_2^+$ species are isolable in the solid phase under proper experimental conditions and if combined with suitable counteranions.

References and Notes

- (1) (a) Christe, K. O.; Wilson, W. W.; Sheehy, J. A.; Boatz, J. A. *Angew. Chem., Int. Ed. Engl.* **1999**, *38*, 2004. (b) Vij, A.; Wilson, W. W.; Vij, V.; Tham, F. S.; Sheehy, J. A.; Christe, K. O. *J. Am. Chem. Soc.* **2001**, *123*, 6308.
- (2) Bernhardt, I.; Drews, T.; Seppelt, K. *Angew. Chem., Int. Ed. Engl.* **1999**, *38*, 2232.
- (3) Stülzle, D.; O'Bannon, P. E.; Schwarz, H. *Chem. Ber.* **1992**, *125*, 279.
- (4) Kerkines, I. S. K.; Papakondylis, A.; Mavridis, A. *J. Phys. Chem. A* **2002**, *106*, 4435.
- (5) Moore, C. E. *Atomic Energy Levels*; NRSDDS-NBS, Circular No.35, U.S. GPO: Washington, DC, 1971.
- (6) Papakondylis, A.; Kerkines, I. S. K.; Mavridis, A. *J. Phys. Chem. A* **2004**, *108*, 11127.
- (7) Westmore, B. J.; Buchanon, W. D.; Plaggenborg, L.; Wenclawiak, B. W. *J. Am. Soc. Mass Spectrom.* **1998**, *9*, 29.
- (8) (a) Raghavachari, K.; Trucks, G. W.; Pople, J. A.; Head-Gordon, M. *Chem. Phys. Lett.* **1989**, *157*, 479. (b) Bartlett, R. J.; Watts, J. D.; Kucharski, S. A.; Noga, J. *Chem. Phys. Lett.* **1990**, *165*, 513. (c) *Chem. Phys. Lett.* **1990**, *167*, 609E.
- (9) (a) Knowles, P. J.; Hampel, C.; Werner, H.-J. *J. Chem. Phys.* **1993**, *99*, 5219. (b) *J. Chem. Phys.* **2000**, *112*, 3106E.
- (10) Dunning, T. H., Jr. *J. Chem. Phys.* **1989**, *90*, 1007.
- (11) MOLPRO is a package of ab initio programs designed by Werner, H.-J.; Knowles, P. J. MOLPRO version 2002.6. Amos, R. D.; Bernhardsson, A.; Berning, A.; Celani, P.; Cooper, D. L.; Deegan, M. J. O.; Dobbyn, A. J.; Eckert, F.; Hampel, C.; Hetzer, G.; Knowles, P. J.; Korona, T.; Lindh, R.; Lloyd, A. W.; McNicholas, S. J.; Manby, F. R.; Meyer, W.; Mura, M. E.; Nicklass, A.; Palmieri, P.; Pitzer, R.; Rauhut, G.; Schütz, M.; Schumann, U.; Stoll, H.; Stone, A. J.; Tarroni, R.; Thorsteinsson, T.; Werner, H.-J. (12) Carrington, A.; Ramsey, D. A. *Phys. Scr.* **1982**, *25*, 272.
- (13) Huber, K. P.; Herzberg, G. H. *Molecular Spectra and Molecular Structure, Vol. IV, Constants of Diatomic Molecules*; Van Nostrand Reinhold: New York, 1979.
- (14) Papakondylis, A.; Mavridis, A. *J. Phys. Chem. A* **1999**, *103*, 1255.
- (15) Kerkines, I. S. K.; Čársky, P.; Mavridis, A. submitted.